Urban Vegetation, Urban Heat Islands and Heat Vulnerability Assessment in Melbourne, 2018

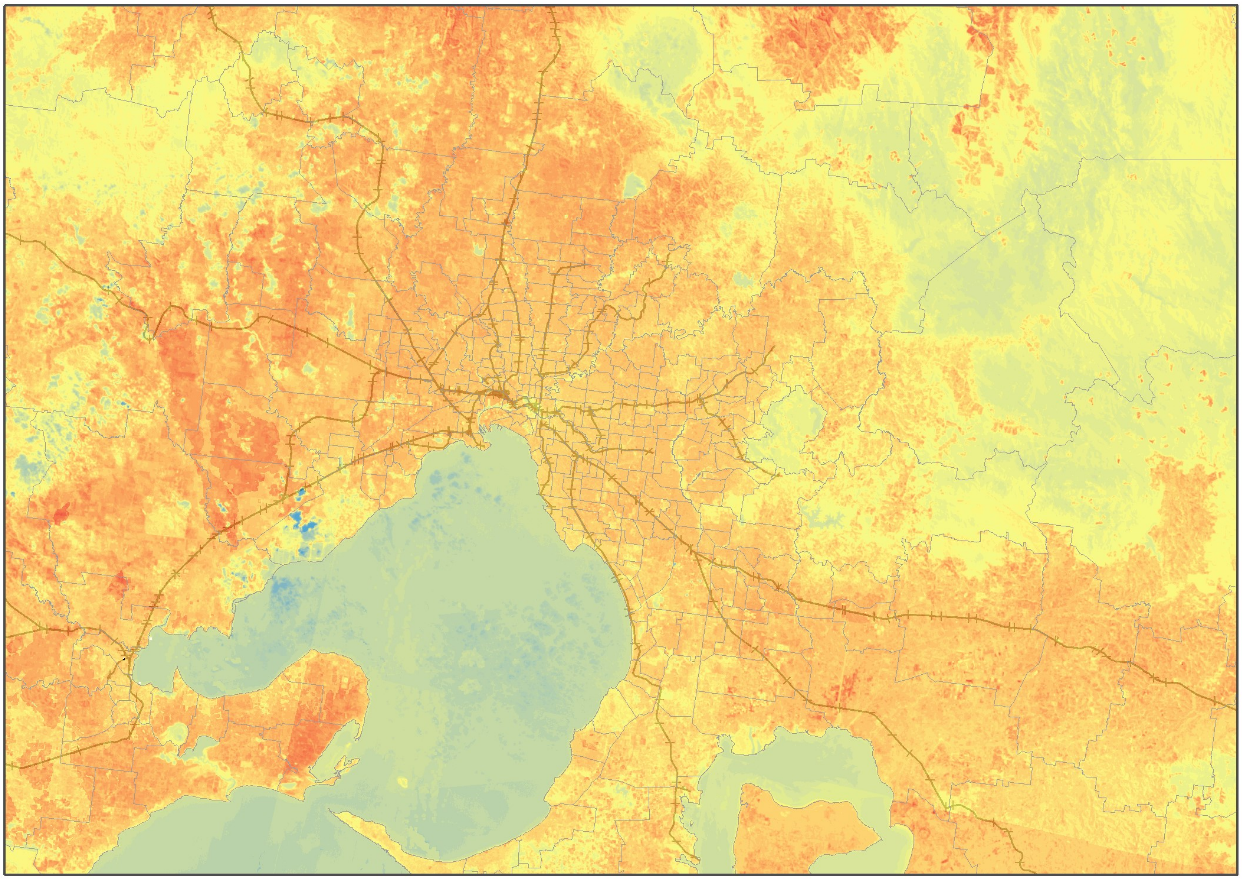

Date: 15/04/2019

Project: Metropolitan monitoring and analysis of vegetation cover, heat and land use

Client: Department an Environment, Land, Water and Planning, Victorian Government

Suggest Citation

Sun C, Hurley J, Amati M, Arundel J, Saunders A, Boruff B, Caccetta P (2019) *Urban Vegetation, Urban Heat Islands and Heat Vulnerability Assessment in Melbourne, 2018.* Clean Air and Urban Landscapes Hub, Melbourne, Australia

Contents

Executive summary 2

Introduction 4

Approach 4

Results: 5

1. **Descriptive Statistics** 5
   1.1. Mesh block level 6
   1.2. LGA level 6
   1.3. Spatial variation and the clusters of UHI: 7
2. **Relationship analysis** 8
   2.1. Global correlations between LST and urban vegetation 8
   2.2. Global regressions for LST and urban vegetation 9
      2.2.1. Simple linear regression for LST and each vegetation types or combinations 9
      2.2.2. Multiple linear regression for LST and the combination of all vegetation types 9
   2.3. Geographically Weighted Regression (GWR) for LST(UHI) and urban vegetation 10
3. **Vulnerability Assessment** 12
4. **Further work: Identifying areas for heat mitigating** 15

References 15

Appendices 18

Executive summary

This report provides a statistical analysis of the relationship between urban vegetation cover and urban heat island effect (UHI) in Melbourne metropolitan area, based on 2018 vegetation cover and land surface temperature data. Both the vegetation and UHI data were attributed to ABS 2016 census Mesh Blocks. This report also presents a heat vulnerability assessment at the SA1 (Statistical Area 1) level, making use of 2016 Census data along with the 2018 vegetation cover and land surface temperature data. The report provides an updated assessment of the relationship between UHI and vegetation cover, and an updated HVI, from the previously submitted interim report based on 2014 vegetation cover and land surface temperature data (Sun et al., 2018). The 2014 and 2018 temperature analysis are not directly compared in this project, as land surface temperature derived from Landsat thermal images is subject to the availability of satellite images, which causes significant annual variation between two different years due to climatic factors which are difficult to control for.

The vegetation structure data was produced using CSIRO's Urban Monitor^{TM} approach (Caccetta *et al*, 2018). This provides a three dimensional representation of the spatial distribution of vegetation at 30 centimetre resolution. Vegetation cover was grouped into five height classes: grass (0-0.5m); shrub (0.5-3m); small tree (3-10m); medium tree (10-15m); large tree (15m+).

The UHI is a measure of the deviation of urban temperatures relative to a non-urban baseline. The UHI measure was derived from land surface temperature (LST) data based on Landsat 8 thermal infrared data collected by the United States Geological Survey (USGS). This data provides a two dimensional representation of the spatial distribution of UHI at 30-meter resolution landscape (Devereux, & Caccetta, 2017).

Summary of LST results:

- Results show that mean UHI LST (UHI_2018_m) varied from 10.20°C to -7.16°C at Mesh Block level.
- Four LGAs have over 9.5°C mean composite summer UHI (Brimbank, Casey, Melton, Moonee Valley).
- With the exception of Mornington Peninsular, Yarra Ranges and Nillumbik, all urban LGAs had over 7.0°C mean composite summer UHI.
- Large UHI concentration areas appeared in the west and southeast part of Melbourne metropolitan, along with some scattered areas with strong UHI effects in the northern suburbs. Lower LST concentration areas were mainly along the coastal areas, eastern and north eastern suburbs and highly vegetated areas.

Global (classic statistical) relationships:

- UHI had weak negative global correlations with percentage of grass and shrub covers.
- UHI has medium global correlation with all other measures of vegetation covers; with the strongest negative correlation being with percentage of total tree cover.
- Both simple regression models and multiple regression models show weak to moderate negative relationships ($R^2 < 0.40$) between UHI and urban vegetation types.

- Therefore, analysis of the global relationship between UHI and vegetation confirms that vegetation is related to reduced UHI, but does not reveal the spatial variation of the relationship.

Local (spatially explicit) relationships:

- When considering the spatial variation in the relationship among LST and vegetation (using Ordinary Least Squares (OLS) and Geographically Weighted Regression (GWR)) we found that tree types are better predictors of UHI than grass and shrub vegetation cover UHI. When local area effects are considered, the combined all vegetation structure is a useful predictor of the UHI with R^2=0.90.

Heat Vulnerability

- High-risk areas with Heat Vulnerability Index (HVI) 5 were mainly distributed in the suburban areas of Melton, Brimbank, Darebin, Casey, Wyndham LGAs. The risks in some areas were high, despite the lower magnitude of UHI, because of the high human sensitivity or lower adaptive capability to heat, such as the SA1s in north Dandenong and Casey.
- Implications: The impact of UHI effects were weakened due to the low social vulnerability in some suburban areas benefitting from the low proportion of sensitive population or the high level of socioeconomic development, such as Nillumbik and some SA1s in Manningham LGAs. By contrast, high social vulnerability intensifies heat health risks in some newly urbanised areas of Melbourne, such as Tarneit and Altona North.

Introduction

Temperatures in many urban areas are warmer than their rural surroundings. This phenomenon is known as the 'Urban Heat Island' which refers to temperature differences attributable to urbanisation. Urban heat islands can have multiple impacts on health, resource use, and air quality. In the absence of a dense network of meteorological stations to measure air temperature, satellite thermal infrared imagery is commonly used to estimate land surface temperatures (LST) instead. Land surface temperatures are most similar to near-ground air temperatures early in the morning. In most situations, however, land surface temperatures are useful for gauging the level of exposure to urban heat, even if there is not always a direct relationship with air temperature. In response to growing heat vulnerability of our urban dwellers, a body of research has sought to identify the causes of warming in urban areas and determine how increasing temperatures manifest as the urban heat island effect (Mirzaei, 2015).

The correlation between urban green space and cooler urban temperatures has been established. However, detecting this correlation does not provide the specific information urban planners require to effectively utilise and develop urban green space as an adaptive strategy to protect urban dwellers from heat. First, this correlation is often observed using vague definitions of green space including broad categorisations of green space itself (Estoque, Murayama, & Myint, 2017), the use of remotely sensed normalised difference vegetation index (NDVI) values (Chun & Guldmann, 2014; Guo et al., 2015), or simply comparing urban surface temperatures with vegetated areas a short distance from urban areas (Zhou, Zhang, Li, Huang, & Zhu, 2016). Variation in the categorisation of green space can obscure the diversity of vegetation in urban areas; or can identify relationships between vegetation and cooling in rural areas which may not translate effectively to urban environments. Wang, Zhan, and Ouyang (2017) also highlight the limitations with existing categorisations of built-up areas and the relationship with temperature. The result is that urban planners lack information concerning how the spatial arrangement and structure of urban vegetation can be used to generate local cooling effects.

This report provides a statistical analysis of the relationship between high resolution urban vegetation cover and satellite derived urban heat island effect (UHI) in Melbourne via both classic and spatial explicit statistical approaches. The report provides an updated assessment of the relationship between UHI and vegetation cover, and an updated HVI, from the previously submitted interim report based on 2014 vegetation cover and land surface temperature data (Sun et al., 2018). The 2014 and 2018 temperature analysis are not directly compared, as land surface temperature measurement is subject to the availability of satellite thermal images, e.g., Landsat-8 has a 16-day revisit cycle, which caused significant annual variation between different years due to climatic factors which are difficult to control for.

Approach

Aim: Analyse the relationships between urban vegetation structure (cover and height of the tree, shrub, and grass) and UHI.

Vegetation data:

The vegetation cover data was produced using CSIRO's Urban Monitor approach (Caccetta *et al*, 2018). This provides a three-dimensional representation of the spatial distribution of vegetation at 20 centimetre resolution. Vegetation cover was grouped into five height classes: grass (0-0.5m); shrub (0.5-3m); small tree (3-10m); medium tree (10-15m); large tree (15m+).

UHI data:

The UHI is a measure of the deviation of urban temperatures relative to a non-urban baseline. The UHI measure was derived from land surface temperature (LST) data based on Landsat 8 thermal infrared data collected by the United States Geological Survey (USGS). This data provides a two dimensional representation of the spatial distribution of UHI at 30-meter resolution landscape (CSIRO, Thermal client report 2017).

The Landsat 8 thermal infrared data used for this study were collected by the USGS at approximately 9.50 AM Eastern Standard Time (EST); 10:50 AM Daylight Saving Time (DST). Only images in summer 2017–18 that were cloud free across all of metropolitan Melbourne were included in this project. The UHI is a measure of the deviation of urban temperatures relative to a non-urban baseline. Native vegetated sites were used to establish the baseline. This was achieved by estimating a first-order fit to the temperature of native vegetation within and around each urban centre. This fit captures any broad-scale temperature trend that is likely independent of urbanisation, such as cooling with increased latitude or proximity to the coast. After subtracting this fit, the residuals may be interpreted as showing finer scale deviations from this trend, including deviations attributable to urbanisation of the landscape (CSIRO, Thermal client report 2017).

Analysis:

We analysed and quantified Landsat-8 derived Land Surface Temperature (LST) and vegetation types (Urban Monitor data) to investigate their relationship for total 55603 Mesh Blocks in Melbourne. Both datasets were corresponding to the year of 2018. The average difference in summer LST (UHI_2018_m) to baseline LST was used as the dependent variable. Both UHI and vegetation data were attributed to ABS 2016 Mesh Block boundary (GIS shapefile layer).

Eight explanatory fields were set up:

PerGrass: Percentage of Grass
PerShrub: Percentage of Shrubs
PerTr3_10m: Percentage of Tree with height from 3 to 10 meters
PerTr10_15: Percentage of Tree with height from 5 to 15 meters
PerTr15mPl: Percentage of Tree with height over 15 meters
PerAnyVeg: Percentage of all vegetation (Grass, Shrubs, Trees)
PerAnyTree: Percentage of all Tree types
PerTrAndSh: Percentage of all Tree types and Shrubs
UHI_2018_m: Average difference in Land Surface Temperature (LST) to baseline LST

We integrated indicators of heat vulnerability to calculate a Heat Vulnerability Index (HVI) at SA1 level. The index consists of three component layers: heat exposure, sensitivity to heat, and adaptive capability. Integration was accomplished by summing the scores from the three vulnerability components, dividing the SA1s into quintiles, and attributing SA1s with a *Heat Vulnerability Rating* scaled from 1 to 5.

Results:

1. Descriptive Statistics

The descriptive statistics help understand the distribution of the variables used across different geographical levels.

1.1. Mesh Block level:

The eight explanatory fields listed above were attributed to the Spatial dataset of ABS Mesh Blocks across Melbourne metro area, subject to vegetation data availability (coverage of 2018 aerial imagery), n=55603.

Across the whole dataset: Results show that mean UHI LST (UHI_2018_m) varied from 16.89°C to -8.92°C at Mesh Block level (Table 1). The mean temperature was 8.36 °C above baseline LST.

Table 1. Mean and Std of UHI_2018 and urban vegetation types for total 55603 Mesh Blocks

	N	Minimum	Maximum	Mean	Std. Deviation	Skewness		Kurtosis	
	Statistic	Statistic	Statistic	Statistic	Statistic	Statistic	Std. Error	Statistic	Std. Error
PerGrass	55603	0.00	94.42	12.2166	11.21015	2.443	0.010	7.924	0.021
PerShrub	55603	0.00	37.57	6.5293	3.13384	0.664	0.010	4.511	0.021
PerTr03_10	55603	0.00	54.36	9.3492	5.42745	0.883	0.010	2.127	0.021
PerTr10_15	55603	0.00	39.52	2.4252	3.08840	2.513	0.010	9.343	0.021
PerTr15Pl	55603	0.00	71.61	1.5239	4.24101	6.069	0.010	47.956	0.021
PerAnyTree	55603	0.00	79.17	13.2983	10.00905	1.688	0.010	4.062	0.021
PerShrbTre	55603	0.00	82.62	19.8276	11.06801	1.187	0.010	2.616	0.021
PerAnyVeg	55603	0.00	97.59	32.0441	15.82258	1.015	0.010	1.608	0.021
UHI_2018_m	55603	-8.92	16.89	8.3571	2.18003	-1.019	0.010	3.881	0.021

1.2. LGA level:

The bar chart in Figure 1 shows, at the LGA level, the average difference in Land Surface Temperature (LST) to baseline LST. When aggregated to LGA, mean UHI LST (UHI_2018_m) varied from 0.03°C to 10.75°C. Four LGA have over 9.5°C mean UHI (Brimbank, Casey, Melton, Moonee Valley). Note that some urban fringe LGAs only contain part of the LGA area due to the vegetation cover data availability. For a detailed breakdown of LGA statistics see **Appendix 1** for data table and box plots).

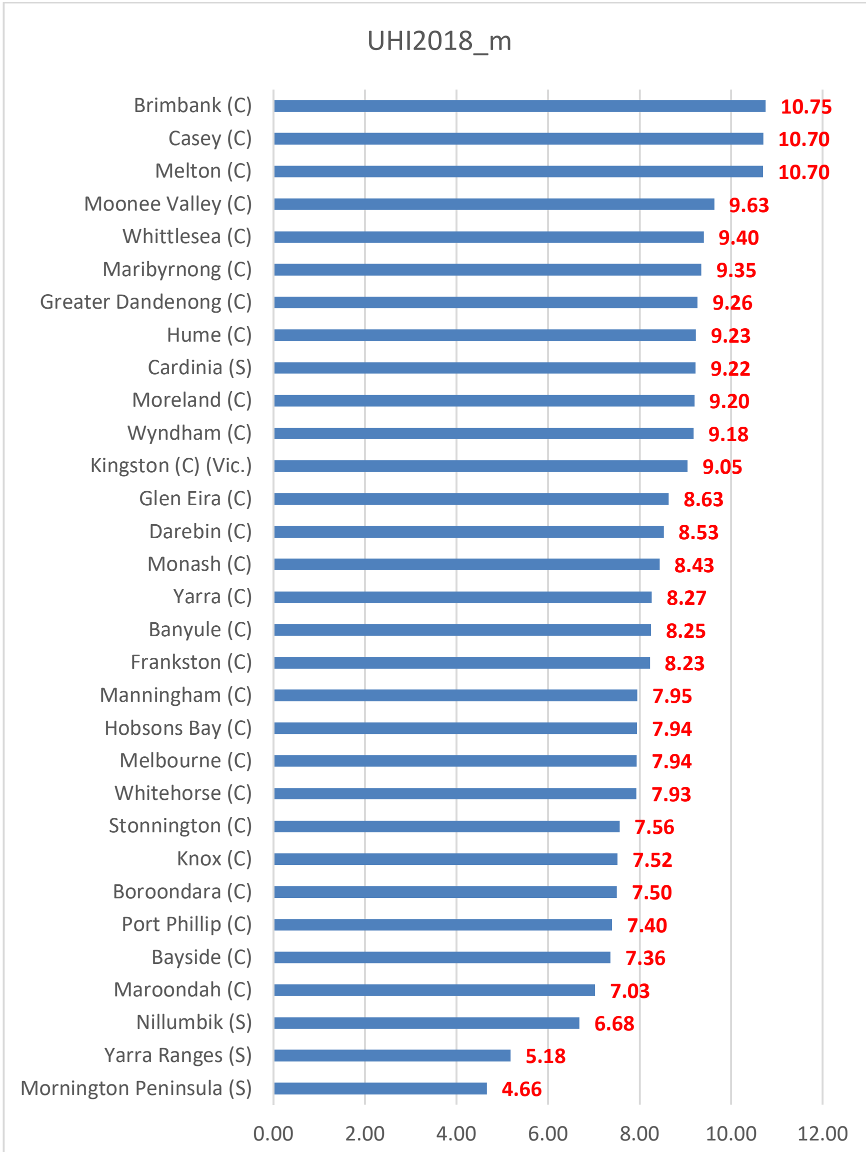

Figure 1. The average difference (°C) in Land Surface Temperature (LST) to baseline LST (°C) between LGAs (LGA_name 2016)

1.3. Spatial variation and the clusters of UHI:

The sum of UHI effects at LGA level (Figure 1) present an average value for overview. They do not indicate the specific areas with significant UHI effects. The spatial pattern of UHI was investigated using Local Moran's I, a spatial statistical method, to identify clusters of UHI at Mesh Block level (Figure 2). The red areas indication regions where high value (mean UHI) areas are next to other high values. UHI large concentration areas appeared in the west (e.g. Melton) and southeast (e.g. Casey) part of Melbourne metropolitan, along with some scattered areas with strong UHI effects in the northern suburbs. Lower LST concentration areas were mainly along the coastal areas, Yarra Valley and highly vegetated areas. The red areas represent regions most effected by UHI, as there is a significant concentration of UHI at Mesh Block level. Therefore, these areas may be appropriate to target with initiatives to reduce UHI.

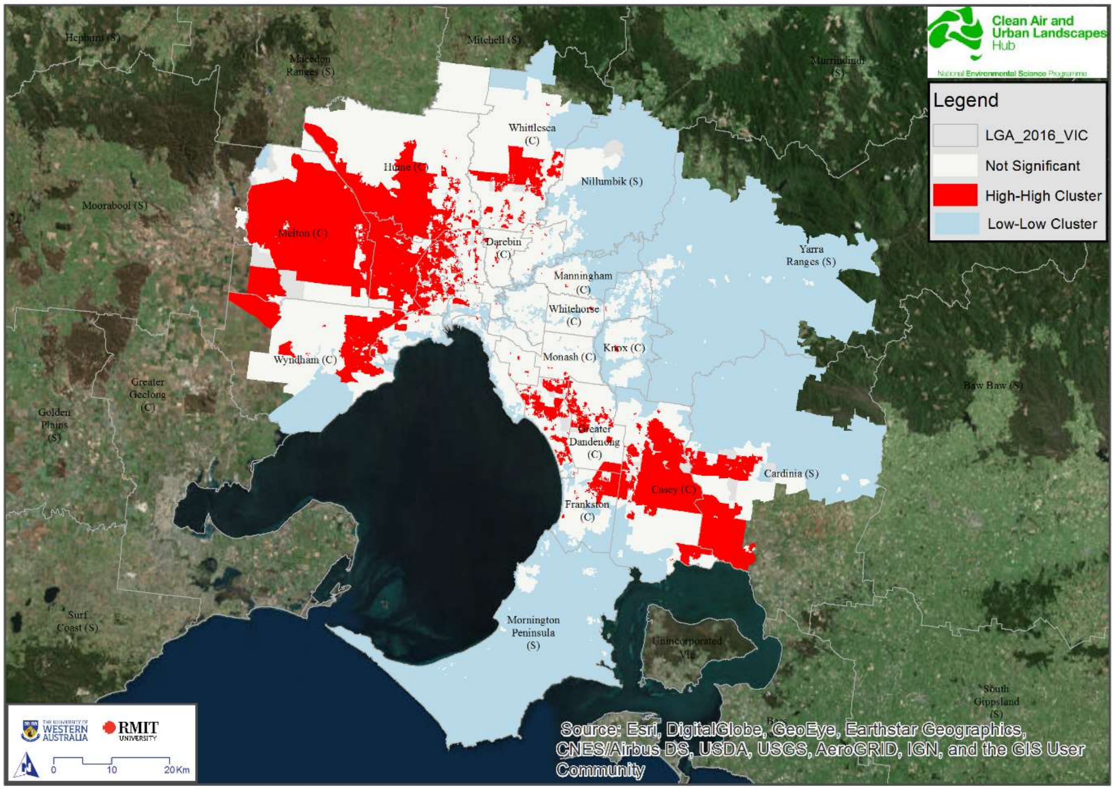

Figure 2. Map of UHI concentration areas in Melbourne metropolitan based on landsat-8 derived LST

2. Relationship analysis

2.1. Global correlations between LST and urban vegetation

Pearson Correlation statistics were performed to explore the strength of the associations between vegetation structure variables and LST (Table 2). Eight vegetation structure variables (percentage of Grass, Shrubs, Trees with three different heights, all vegetation, all trees, Shrubs& all Trees in each Mesh Block) and the average difference in summer LST (UHI_2018_m) to baseline LST were used for analysis in SPSS.

Table 2. Pearson Correlation coefficients between UHI_2018 and urban vegetation types

		PerGrass	PerShrub	PerTr3_10m	PerTr10_15	PerTr15mPl	PerAnyVeg	PerAnyTree	PerTrAndSh
UHI_2018_m	Pearson Correlation	-.034**	-.162**	-.474**	-.451**	-.447**	-.426**	-.585**	-.575**
	Sig. (2-tailed)	0.000	0.000	0.000	0.000	0.000	0.000	0.000	0.000
	N	55603	55603	55603	55603	55603	55603	55603	55603

** Correlation is significant at the 0.01 level (2-tailed).
** Correlation is significant at the 0.01 level (2-tailed).

UHI_2018_m has inverse correlations with the eight fields, with strongest coefficient (r) of 0.585 for PerAnyTree.

This shows:

- Grass has a weak negative impact on UHI (r =-0.034).
- Shrub has weak negative impact on UHI (r = -0.162).
- All individual tree types have medium negative impact on UHI (-0.4 > r > -0.5).
- All trees and shrubs&trees have medium negative impact on UHI (r <-0.5).
- Therefor in terms of reducing UHI, it is trees that would have the most impact, whereas shrubs minor and grass very little.

2.2. Global regressions for LST and urban vegetation

Simple and multiple linear regressions were performed to examine the relationships between average difference in LST to baseline LST (dependent variable) and urban vegetation structures (independent variables) in order to estimate the causal effects of vegetation on LST or to predict how effective urban vegetation can be to reduce the LST.

2.2.1.Simple linear regression for LST and each vegetation types or combinations

Dependent variable: UHI_2018_m
Independent variables: PerGrass; PerShrub; PerTr3_10m; PerTr10_15; PerTr15mPl; PerAnyVeg; PerAnyTree; PerTrAndSh.

Simple Regression Results/observation: Scatter plots in **Appendix 2** (Figure s4 – Figure s11)

"AnyTree" is observed as the best predictor of the explanatory variables (R^2 =0.34), however, under simple linear it is a weak predictor of reduced UHI.

2.2.2.Multiple linear regression for LST and the combination of all vegetation types

Dependent variable: UHI_2018_m
Independent variables: PerGrass; PerShrub; PerTr3_10m; PerTr10_15; PerTr15mPl

SPSS Regression method: Enter

The outputs from the multiple linear regression are in Table 3 and 4. As with single regression, multiple regression finds the combination of vegetation types is a weak predictor of UHI (R^2 = 0.356). We expect that these weak relationship is partly due to geographical factors, in particular distance decay. For example, patches of small and isolated vegetation are not likely to influence UHI; whereas agglomerations of vegetation and tree patches are more likely to impact UHI.

Table 3. Summary of Multiple linear regression model

Model	R	R^2	Adjusted R^2	Std. Error of the Estimate
1	.597[a]	0.356	0.356	1.74901

a. Predictors: (Constant), PerTr15mPl, PerGrass, PerTr3_10m, PerShrub, PerTr10_15

Table 4. Coefficients of multiple linear regression model

Coefficients[a]						
		Unstandardized Coefficients		Standardized Coefficients		
Model		B	Std. Error	Beta	t	Sig.
1	(Constant)	10.322	0.02		520.939	0.00
	PerGrass	-0.012	0.001	-0.062	-17.313	0.00
	PerShrub	-0.006	0.003	-0.009	-2.175	0.03
	PerTr3_10m	-0.154	0.002	-0.383	-74.395	0.00
	PerTr10_15	-0.028	0.004	-0.04	-7.414	0.00
	PerTr15mPl	-0.177	0.002	-0.344	-81.618	0.00

a. Dependent Variable: UHI_2018_m

2.3. Geographically Weighted Regression (GWR) for LST (UHI) and urban vegetation

Geographically Weighted Regression (GWR) is a technique for exploratory data analysis that provides estimates of regression coefficients for each geographical location, based on a weighting of other observations near that location. The basic assumption is that observations exhibit spatial dependency: in some areas the influence might be much stronger than in other areas. This has its root from the first law of geography "Everything is related to everything else, but near things are more related than distant things". The geographically weighted regression (GWR) method, a spatial form of linear regression, analyses spatial relationships between variables. GWR is more effective than global regression at exploring the spatially varied relationship between LST and vegetation variables.

Ordinary Least Squares (OLS) regression, serves as a starting point to select the key explanatory variables. OLS is similar to linear regression but gives the maximum likelihood estimation on the relationships between dependent and independent variables. It is also used to measure the variables' multicollinearity with the variance inflation factor (VIF).

Observations from the OLS and GWR results:
OLS results (Table 5) show that all vegetation types have negative relationships with UHI effect, although both grass and shrub are very poor predictors for UHI effect ($r < 0.01$). In addition, no significant multicollinearity was found between the explanatory variables (VIFs are moderate). We then used all the five vegetation types as explanatory variables to build a GWR model. Results of GWR (Table 6) show that the model achieved adjusted R^2=0.90, which indicates that LST difference in 90% of studied Mesh Blocks was explained by the combination of three types of vegetation. R-Squared is a measure of goodness of fit. Its value varies from 0.0 to 1.0, with higher values being preferable. It may be interpreted as the proportion of dependent variable variance accounted for by the regression model.

Table 5. OLS observations

Variables	Coefficients	*p*	VIF
PerGrass	-0.0121	0.00	1.11
PerShrub	-0.0064	0.03	1.55
PerTr3_10m	-0.1539	0.00	2.29
PerTr10_15	-0.0279	0.00	2.45
PerTr15mPl	-0.1767	0.00	1.53

Table 6. GWR report on R^2

	OBJECTID *	VARNAME	VARIABLE	DEFINITION
▸	1	Neighbors	100	
	2	ResidualSquares	20036.085101	
	3	EffectiveNumber	10198.675105	
	4	Sigma	0.666688	
	5	AICc	118971.667534	
	6	R2	0.922734	
	7	R2Adjusted	0.905254	
	8	Dependent Field	0	UHI18_m
	9	Explanatory Field	1	PerGrass
	10	Explanatory Field	2	PerShrub
	11	Explanatory Field	3	PerTr03_10
	12	Explanatory Field	4	PerTr10_15
	13	Explanatory Field	5	PerTr15Pl

To examine the spatial weighted influence of vegetation cover structure the GWR model generates local estimates (coefficients and R^2) for the dependent variable (UHI). The spatial changes in the magnitude of the R^2 parameter indicate the locally changing influence of tree cover structure on the dependent variable, here the UHI (see Figure 3). This is the essence of spatial heterogeneity: the structure of the model changes from place to place across the study area as the parameter estimates change in relation to each other in the model. Local R^2 range between 0.0 and 1.0 indicating how well the local regression model fits observed UHI values. Very low values indicate the local model is performing poorly. Mapping the Local R^2 values to see where GWR predicts well and where it predicts poorly may provide clues about important variables that may be missing from the regression model.

The GWR model also generates the local coefficients for independent variables. The coefficients for the individual contribution of the three different vegetation classifications (grass, shrubs, tree 3-10m; tree 10-15m; tree 15+) to the UHI effect are included in **Appendix 3**). The effects vary between different types and across different locations. In practical terms the local estimates can be used for mitigating strategies. The results also recognise that small and isolated patches of vegetation are less likely to influence temperature (expect perhaps at very local scale and undetectable by satellite), than consolidated patches.

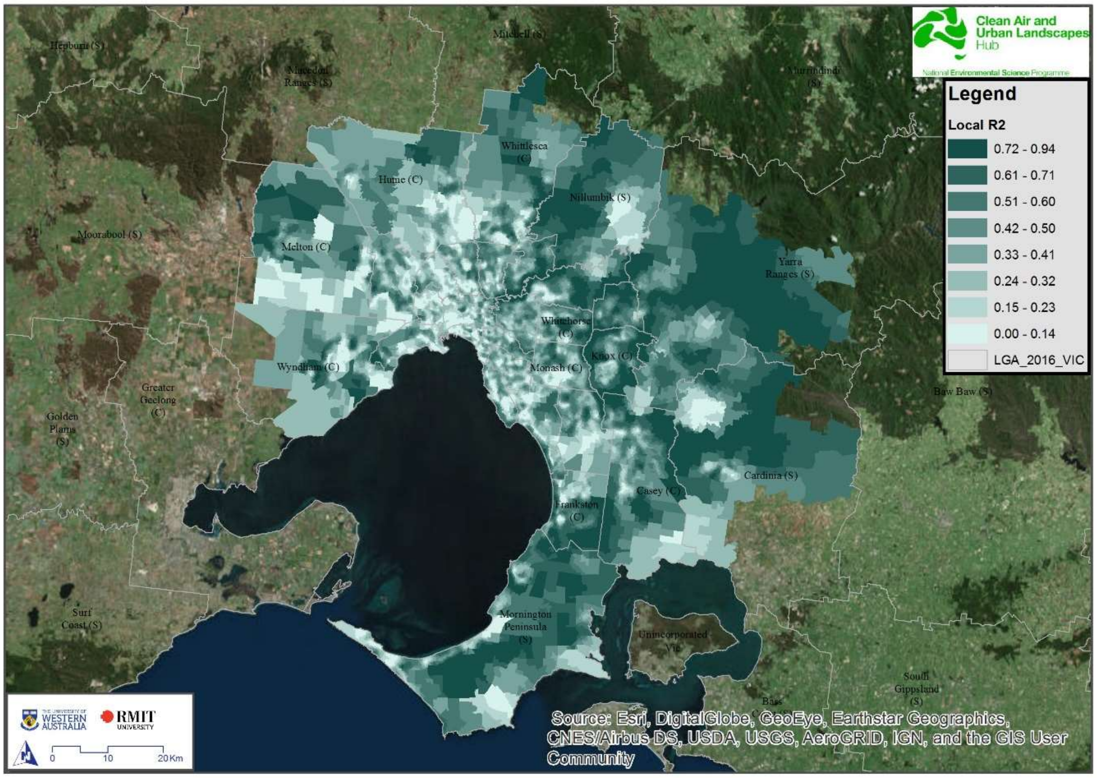

Figure 3. Local R^2 of GWR analysis between vegetation types and LST in Melbourne. darker colour indicates high goodness-of-fit.

3. Vulnerability Assessment

The heat vulnerability assessment is to identify areas where we might expect high vulnerability to heat waves. We focus on areas with higher UHI relative to baseline; in combination with selected land cover attributes and demographic characteristics. Table 7 shows the breakdown indicators for calculate the Heat Vulnerability Index (HVI).

In the absence of a dense network of meteorological stations to measure air temperature, satellite thermal infrared imagery is commonly used to estimate land surface temperatures (LST) instead. Land surface temperatures are most close to near-ground air temperatures early in the morning. In most situations, land surface temperatures are useful for gauging the level of exposure to urban heat (Inostroza, Palme, & de la Barrera, 2016). We used LST derived UHI for heat exposure indicator. It is also acknowledged that socioeconomic factors play an important role in the ability of populations to prepare for, respond to, and recover from heat and their vulnerability (Rohat et al., 2019; Wilhelmi & Hayden, 2010).

Land cover provides a sensitivity indicator for the retention of heat in the urban environment.

- Following above analysis of vegetation impact of UHI, we used % trees as a sensitivity indicator, with high cover corresponding with a low sensitivity score.
- We used % roads as a sensitivity indicator, with high cover corresponding with a high sensitivity score, as roads retain heat in the urban environment.
    - Note: % built up area is commonly used as a sensitivity indicator. If DELWP can provide building footprint data, this can be included in the analysis.

Demographic data:

- We used population density (persons per square km) as a sensitivity indicator, with high number corresponding with a high sensitivity score, as denser populations are more sensitive to heat related health complications.
- We used population (Percentage) of people >= 65 years old as a sensitivity indicator, with high number corresponding with a high sensitivity score, as elderly people are more sensitive to heat related health complications.
- We used population (Percentage) of people <= 4 years old as a sensitivity indicator, with high number corresponding with a high sensitivity score, as very young people are more sensitive to heat related health complications.
- We used persons in need of care as a sensitivity indicator, with high number corresponding with a high sensitivity score, as persons needing care are more sensitive to heat related health complications.
- We used SEIFA-IRSD as an adaptive indicator, with high deciles corresponding with a high adaptive capacity score, as more advantaged populations have more resources to respond to heat.

  We used SEIFA-IEO as an adaptive indicator, with high deciles corresponding with a high adaptive capacity score, as more advantaged populations have more resources to respond to heat.

Table 7. Indicators of exposure, sensitivity and adaptive capacity for heat vulnerability index

Exposure Indicator	Sensitivity Indicators						Adaptive capacity indicators	
UHI	Vegetation	Roads	Population density	Elderly	Very young	Persons need care	SEIFA-IRSD	SEIFA-IEO
A) Assign each SA1 mean UHI based on meshblocks; Normalise to 0-1 range.	**B**) Assign each SA1 mean cover based on meshblocks; Normalise to 0-1 range.	**C**) Assign each SA1 mean cover based on meshblocks; Normalise to 0-1 range.	D) Assign each SA1 mean population density based on meshblocks; Normalise to 0-1 range.	**E**) Assign each SA1 mean elderly population based on meshblocks; Normalise to 0-1 range.	**F**) Assign each SA1 mean very young population based on meshblocks; Normalise to 0-1 range.	**G**) Assign each SA1 mean Persons need care based on meshblocks; Normalise to 0-1 range.	**H**) Socio-economic index score; Normalise to 0-1 range.	**I**) Eucational and occupational level index score; Normalise to 0-1 range.
= A	**= (B+C+D+E+F+G)/6**						**=(H+I)/2**	

Exposure indicator into Quintiles
Sensitivity Indicators into Quintiles
Adaptive capacity indicators into Quintiles

Sum aggregated indicators to determine vulnerability score. This gives equal weighting (one third each) to exposure, sensitivity, and adaptability.

Heat Vulnerability Index = Exposure Index + Sensitivity Index– Adaptive Capacity Index

HVI 1 = First quintile (1/3 (A + (B+C+D+E+F+G)/6 - (H+I)/2)
HVI 2 = Second quintile (1/3 (A + (B+C+D+E+F+G)/6 - (H+I)/2)
HVI 3 = Third quintile (1/3 (A + (B+C+D+E+F+G)/6 - (H+I)/2)
HVI 4 = Fourth quintile (1/3 (A + (B+C+D+E+F+G)/6 - (H+I)/2)
HVI 5 = Fifth quintile (1/3 (A + (B+C+D+E+F+G)/6 - (H+I)/2)
HVI 0: means that the SA1 has no population in census 2016.

Normalisation and equal weighting for individual variables were used in the calculation with the reference of other studies (Aubrecht & Özceylan, 2013; Chow, Chuang, & Gober, 2012; Dong et al., 2014; Tomlinson, Chapman, Thornes, & Baker, 2011; Vescovi, Rebetez, & Rong, 2005). The original scores of indicators were normalised between 0 and 1 using min-max normalisation, so that the normalized values of variables are relative importance measures of each SA1s in relation to the others.

The assessment of heat vulnerability as SA1 level provides more detailed pattern of spatial heterogeneity than other studies at LGA level. However, the data can be aggregated to SA3 or LGA level.

Figure 3 maps the HVI at SA1 across the study area (HVI 1-5 corresponding to lowest-highest vulnerability to heat). High-risk areas with Heat Vulnerability Index (HVI) 5 were mainly distributed in the suburban areas of Melton, Brimbank, Darebin, Casey, Wyndham LGAs. The risks in some areas were high, despite the lower magnitude of UHI, because of the high human sensitivity or lower adaptive capability to heat, such as the SA1s in north Dandenong and Casey. The impact of UHI effects were weakened due to the low social vulnerability in some suburban areas benefitting from the low proportion of sensitive population or the high level of socioeconomic development, such as Nillumbik and some SA1s in Manningham LGAs. By contrast, high social vulnerability intensifies heat health risks in some newly urbanised areas of Melbourne, such as Tarneit and Altona North.

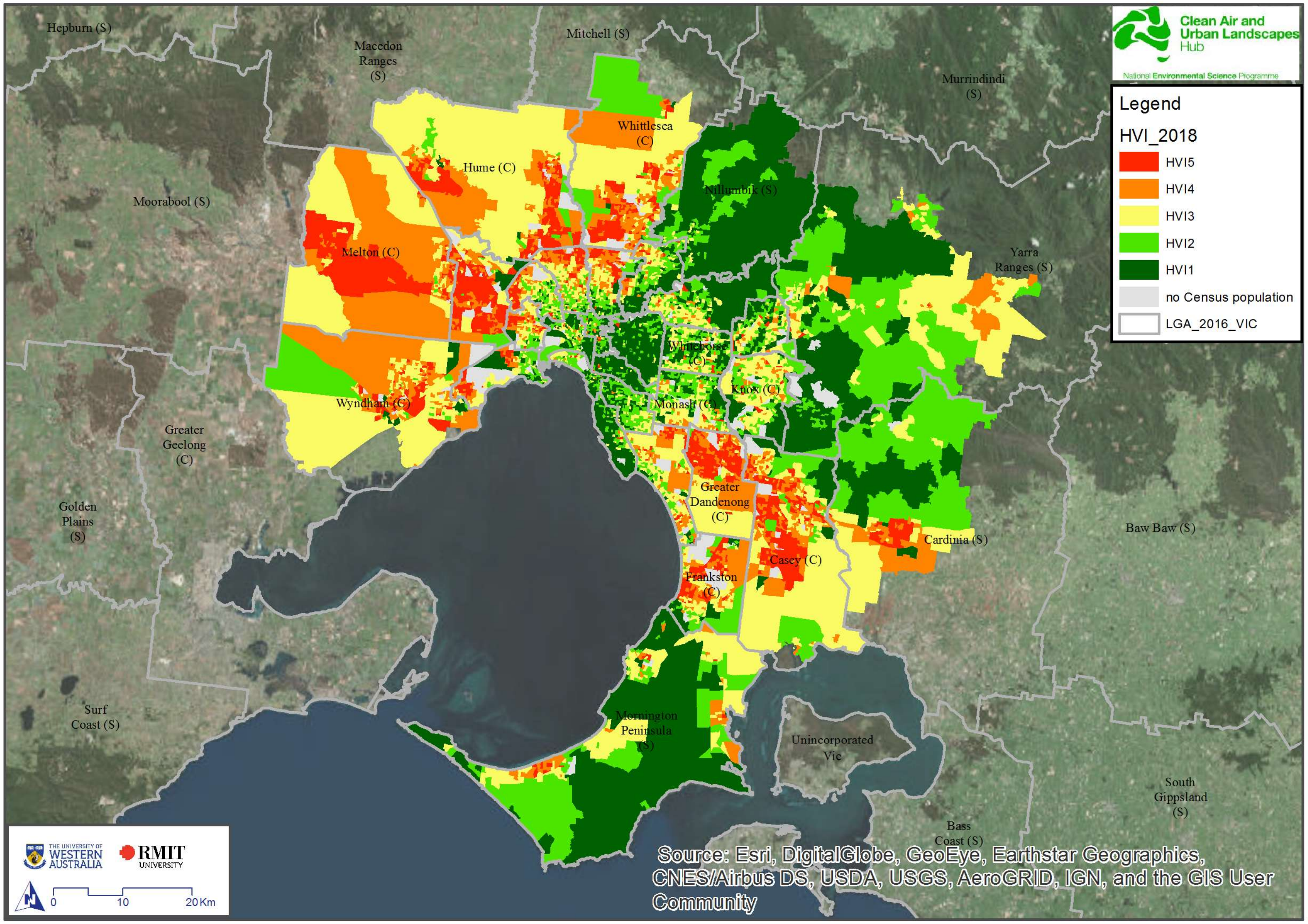

Figure 3. Map of Heat Vulnerability Index (HVI) at SA1 level in Melbourne metropolitan area

4. Further work: identifying areas for heat mitigating

Hot weather is a threat to human health, particularly for vulnerable populations, such as older or very young people in cities. Increased vegetation can help reduce temperatures and exposure to heat hazards. The spatial heterogeneity of heat-related diseases suggests that interventions (e.g. tree planting) should be targeted for maximum impact. Analysing heat vulnerability for communities offers opportunities for presenting information to support decision-making.

The relationships between UHI and vegetation cover are spatially varying and therefore needed to be studied by means of geographically weighted models. To further predict the degree of heat reduction, more variables can be included and PCA (Principal component analysis) can be used to decide the important variables. Likewise, more heat vulnerability indicators can be included and PCA can be used to determine the level of heat vulnerability at local scales by providing insights into these indexes (Bao, Li, & Yu, 2015; Inostroza et al., 2016; Loughnan, 2013).

Taking consideration of both the influence of vegetation on UHI (local R^2 values from GWR) and HVI, we can identify SA1 areas where trees have higher impact on temperature and where the communities are more vulnerable to heat. These are areas to target for potential heat mitigation via increases in tree cover.

The findings in this exercise warn against the simplistic use of global spatial or statistical analysis on available data to target areas for interventions. The approach enables local governments to identify hot spots of vulnerability, and allocate resources such as increased vegetation cover to vulnerable populations.

References

Caccetta et al. (2018). UrbanMonitor®2014 Melbourne. Metropolitan monitoring and analysis of vegetation cover, heat and land use. Department an Environment, Land, Water and Planning, Victorian Government, RMIT University.

Devereux, D., & Caccetta, P. (2017). Estimation of Land Surface Temperature and Urban Heat Island effect for Australian urban centres. Horticulture Innovation Australia (HIA) *Where Should All the Trees Go?* Report EP173542, CSIRO.

Aubrecht, C., & Özceylan, D. (2013). Identification of heat risk patterns in the US National Capital Region by integrating heat stress and related vulnerability. *Environment international, 56*, 65-77.

Bao, J., Li, X., & Yu, C. (2015). The construction and validation of the heat vulnerability index, a review. *International journal of environmental research and public health, 12*(7), 7220-7234.

Chow, W. T., Chuang, W.-C., & Gober, P. (2012). Vulnerability to extreme heat in metropolitan Phoenix: spatial, temporal, and demographic dimensions. *The Professional Geographer, 64*(2), 286-302.

Chun, B., & Guldmann, J.-M. (2014). Spatial statistical analysis and simulation of the urban heat island in high-density central cities. *Landscape and Urban Planning, 125*, 76-88.

Dong, W., Liu, Z., Zhang, L., Tang, Q., Liao, H., & Li, X. e. (2014). Assessing heat health risk for sustainability in Beijing's urban heat island. *Sustainability, 6*(10), 7334-7357.

Estoque, R. C., Murayama, Y., & Myint, S. W. (2017). Effects of landscape composition and pattern on land surface temperature: An urban heat island study in the megacities of Southeast Asia. *Science of the Total Environment, 577*, 349-359.

Guo, G., Wu, Z., Xiao, R., Chen, Y., Liu, X., & Zhang, X. (2015). Impacts of urban biophysical composition on land surface temperature in urban heat island clusters. *Landscape and Urban Planning, 135*, 1-10.

Inostroza, L., Palme, M., & de la Barrera, F. (2016). A heat vulnerability index: spatial patterns of exposure, sensitivity and adaptive capacity for Santiago de Chile. *PLOS ONE, 11*(9), e0162464.

Loughnan, M. E. (2013). *A spatial vulnerability analysis of urban populations during extreme heat events in Australian capital cities*: National Climate Change Adaptation Research Facility.

Mirzaei, P. A. (2015). Recent challenges in modeling of urban heat island. *Sustainable cities and society, 19*, 200-206.

Rohat, G., Flacke, J., Dosio, A., Pedde, S., Dao, H., & van Maarseveen, M. (2019). Influence of changes in socioeconomic and climatic conditions on future heat-related health challenges in Europe. *Global and Planetary Change, 172*, 45-59. doi:https://doi.org/10.1016/j.gloplacha.2018.09.013

Sun C, Hurley J, Amati M, Arundel J, Saunders A, Boruff B, Caccetta P (2018) *Interim Report: Summary Statistical Analysis of the Relationships between Vegetation Class and Urban Heat Island (UHI), Melbourne metropolitan area, Version 2.* Clean Air and Urban Landscapes Hub, Melbourne, Australia

Tomlinson, C. J., Chapman, L., Thornes, J. E., & Baker, C. J. (2011). Including the urban heat island in spatial heat health risk assessment strategies: a case study for Birmingham, UK. *International journal of health geographics, 10*(1), 42.

Vescovi, L., Rebetez, M., & Rong, F. (2005). Assessing public health risk due to extremely high temperature events: climate and social parameters. *Climate Research, 30*(1), 71-78.

Wang, Y., Zhan, Q., & Ouyang, W. (2017). Impact of Urban Climate Landscape Patterns on Land Surface Temperature in Wuhan, China. *Sustainability, 9*(10), 1700.

Wilhelmi, O. V., & Hayden, M. H. (2010). Connecting people and place: a new framework for reducing urban vulnerability to extreme heat. *Environmental Research Letters, 5*(1), 014021.

Zhou, D., Zhang, L., Li, D., Huang, D., & Zhu, C. (2016). Climate–vegetation control on the diurnal and seasonal variations of surface urban heat islands in China. *Environmental Research Letters, 11*(7), 074009.